Avoidance response to CO_2 in the lateral horn

Nélia Varela, Miguel Gaspar, Sophie Dias, Maria Luísa Vasconcelos*

Champalimaud Research, Champalimaud Centre for the Unknown, 1400-038 Lisbon, Portugal

*Corresponding author

ABSTRACT

In flies, the olfactory information is carried from the first relay in the brain, the antennal lobe, to the mushroom body (MB) and the lateral horn (LH). Olfactory associations are formed in the MB. The LH was ascribed a role in innate responses based on the stereotyped connectivity with the antennal lobe, stereotyped physiological responses to odors and MB silencing experiments. Direct evidence for the functional role of the LH is still missing. Here we investigate the behavioral role of the LH neurons directly, using the CO_2 response as a paradigm. Our results show the involvement of the LH in innate responses. Specifically, we demonstrate that activity in two sets of neurons is required for the full behavioral response to CO_2. Using calcium imaging we observe that the two sets of neurons respond to CO_2 in different manners. Using independent manipulation and recording of the two sets of neurons we find that the one that projects to the SIP also outputs to the local neurons within the LH. The design of simultaneous output at the LH and the SIP, an output of the MB, allows for coordination between innate and learned responses.

INTRODUCTION

Animals use the olfactory system to find partners or food and to avoid predators. To a certain extent the ability to navigate the olfactory environment is hardwired. This ability is expanded with life experiences that result in olfactory associations. The architecture of the olfactory system is comprehensively characterized in the fruit fly and it is remarkably similar to the mammalian olfactory system (1,2).

Olfactory sensory neurons express a single odorant receptor. Olfactory sensory expressing the same receptor project to the same glomerulus in the first olfactory center in the brain called antennal lobe in the fly. Most projection neurons innervate a single glomerulus and carry the information to higher brain centers: the mushroom body (MB) and the lateral horn (LH) (3,4). The MB is critical for olfactory associations (5). The LH was ascribed the role of innate response based on MB silencing experiments (6,7). Projection neurons from the antennal lobe connect to the MB without apparent spatial selection whereas at the LH axonal arbors from different glomeruli interdigitate in a stereotyped fashion (3,4,8–11). The stereotypy is consistent with the proposed role for the LH as the center for innate olfactory processing. Though the axonal arbors of projection neurons interdigitate the findings that the arbors of projection neurons that carry information on pheromone and food odors segregate within the LH and that a region within the LH is tuned to repulsive odors suggest dedicated processing areas within the LH (12,13). Lateral horn neurons (LHNs) that respond to the male pheromone 11-cis-vaccenyl acetate were identified based on the expression of the male-specific form of the transcription factor fruitless (14,15). One cluster of male LHNs responds specifically to the pheromone. These results open the possibility that each odor has a cognate LHN. Indeed, a theoretical study supports this connectivity (16). However, activity and anatomy of other LHN clusters suggests a mixed model of connectivity (17). While connectivity at the LH is being scrutinized, direct evidence for the functional role of the LH is still missing.

One of the innate responses with the highest magnitude is the response to CO_2. Unlike most insects *Drosophila melanogaster* avoids CO_2 when tested on a T-maze. The aversive response up to 2% CO_2 is solely mediated by antennal neurons expressing the CO_2 receptor complex GR21a-GR63a which connect to the V glomerulus in the antennal lobe (18,19). Synaptic inhibition of GR21a-GR63a expressing neurons abolishes the avoidance response to low concentrations of CO_2 (20). Conversely, artificial stimulation of CO_2 sensing

neurons with light elicits the avoidance behavior typically observed in response to CO_2 (21). Not all responses to CO_2 are mediated by GR21a-GR63a neurons. Higher CO_2 concentrations elicit a response to acid which is processed in a separate glomerulus (22). Also, a recent study shows that the response to CO_2 is state-dependent with high activity flies moving towards CO_2 and low activity flies avoiding CO_2 (23). The attractive response does not require GR21a-GR63a receptors, instead it is mediated by the ionotropic co-receptor IR25a.

Here we address directly the behavioral role of the LH neurons using the CO_2 avoidance to low concentrations to probe the requirement of the LH for innate responses. We demonstrate that activity in two sets of neurons is required selectively in the behavioral response to CO_2.

RESULTS

Neurons labeled by lines *R21G11* and *R23C09* process CO_2 avoidance

We chose to investigate the role of LH neurons in the context of the response to CO_2 due to the high magnitude of the innate response. To identify neurons involved in CO_2 avoidance we performed an inhibitory screen of fly lines labeling LH neurons (Figure S1). Through visual inspection of the expression pattern of Janelia's collection of *GAL4* lines we selected 32 lines with obvious LH innervation (24,25). To silence the neurons we expressed the inwardly rectifier potassium channel, *Kir2.1* (26), that hyperpolarizes neurons and thus decreases the probability of firing an action potential. In the screen and in other behavioral experiments with *GAL4* lines, we restricted *Kir2.1* expression to adult stage by using a temperature sensitive *GAL80* (*$GAL80^{ts}$*, see materials and methods) (27). The 32 lines were tested on a T-maze where flies were allowed to choose between air and 0.5% CO_2 (Figure S1A). Eight lines showed a significant reduction in avoidance (multiple t-test corrected with Holm-Sidak method, $p<0.05$,) and when retested, three of them exhibited a consistent reduction in

avoidance to CO_2 (Figure S1B). Line *R65D12* was discarded due to innervation in the V-glomerulus (data not shown). Neurons in lines *R21G11* and *R23CO9* (which we will henceforth call *21G11* and *23CO9* neurons) are necessary for the behavioral response to CO_2 (Figure 1A, here tested to 1% CO_2). Since the requirement of the V-glomerulus bilateral projection neurons and the MB for CO_2 avoidance is feeding state dependent (10), we tested if feeding state also affects the contribution of *21G11* and *23C09* neurons in the avoidance response of the fly. We observe that starvation does not alter the phenotype, indicating that the involvement of *21G11* and *23C09* neurons in CO_2 response is independent of the feeding state of the fly (Figure S2A).

Given that CO_2 avoidance is reduced but not abolished for either line we tested flies with both sets of neurons silenced (Figure S2B). We observe no change in the phenotype indicating that the two sets of neurons do not complement each other, i.e., the activity of these populations may not be independent to drive avoidance responses (Post-hoc two-way ANOVA comparing individual and combined expressions not significant both for control and test samples). It has been previously shown that different projection neurons of the V-glomerulus are required for the behavioral response to different CO_2 concentrations (9). Therefore we tested whether the requirement of *21G11* and *23C09* neurons for avoidance to CO_2 was concentration dependent. For this experiment, we used lines *21G11-LexA* and *23C09∩VGlut* that have a restricted expression when compared to *R21G11* and *R23C09* lines (Figure 1D and E, see below). We observe that silencing the activity of these neurons reduces the avoidance behavior of the flies in a comparable manner across odor concentrations (Post-hoc two-way ANOVA comparing across odor concentrations not significant both for control and test samples). These results suggest that *21G11* and *23C09* neurons contribute to CO_2 avoidance independently of concentration (within the range that does not engage the acid sensing response).

Anatomical inspection reveals that line 21G11 labels one cluster of neurons that innervate the dorsoposterior area of the LH and project to the superior intermediate protocerebrum (SIP) (Figure 1D). Some morphological and physiological types of LH output neurons have been described previously (17,28). The *21G11* cluster with its posterior cell bodies and projections to the SIP does not appear to correspond to the described morphological categories.

We generated a *LexA* version of the line to allow independent manipulation of the 21G11 and 23CO9 clusters of neurons. The *LexA* version of 21G11 is very sparse. Additionally, the number of neurons labeled in the LH cluster is smaller. We counted 10 cell bodies in the *LexA* version and 16 to 18 cell bodies in the *GAL4* version (n=5). When we overlaid the expression of both lines we found that 7 to 9 cells were specific to *21G11-GAL4*, three cells specific to *21G11-LexA* and seven cells are common to both lines (Figure S3, n=9). Nevertheless, activity in *21G11-LexA* neurons is necessary to elicit full CO_2 avoidance (see Figure 1C). Line *23C09* labels more than one cluster of neurons at the LH (Figure 1E). To narrow down the expression of line *23C09*, we generated a *splitGAL4* version and then we intersected the expression with that of different neurotransmitter-*splitGAL4* lines (29,30). We found that a glutamatergic cluster located posteriorly is involved in the response (Figure 1C and E). This cluster, which we will call *23C09∩VGlut*, has 8 to 10 cell bodies (n=3) with processes only within the LH. For expression of these lines in 10 μm sections across the brain see Figure S4.

In order to determine the polarity of *21G11* neurons we used the neural compartment markers Dscam17.1-GFP(31), for dendrites and Synaptotagmin-HA (32) for presynaptic areas. Dscam17.1-GFP signal localized exclusively to the LH, which indicates that these neurons receive inputs there, presumably olfactory. The synaptotagmin-HA signal, on the other hand, is localized both to the LH and the SIP. To exclude the possibility that the *GAL4* cluster holds a mix population of neurons with different polarities we marked the more restricted *21G11-LexA* neurons and observed the same distribution of Synaptotagmin-HA (Figure S5). These results suggest that *21G11* neurons output both in the SIP and the LH. Finally, we asked if *21G11* or *23C09* contact projections from the V-glomerulus.

Three distinct projection neurons from the V glomerulus (VPN) at the antennal lobe innervate the medial border of the LH (9,10). We tested two VPNs for which there are lines available with a strong visible projection. We do not see clear overlap at the LH between the innervation of the VPNs and the innervation of the LH neurons we identified (Figure 1H and I). This observation together with the fact that the reduction in avoidance is not complete indicates that additional LH neurons are involved in the response.

21G11 **and** ***23C09 ∩ VGlut*** **neurons respond to CO_2 in different concentration dependent manners**

Having demonstrated that *21G11* and *23C09* neurons are required for the behavioral response to CO_2, we next addressed the physiological response of these neurons. We measured the changes in internal free calcium levels in *21G11* and *23C09∩VGlut* neurons upon stimulation with CO_2. For this we expressed the genetically encoded calcium indicator *GCaMP6m* (33) in *21G11* and *23C09∩VGlut* neurons and recorded the calcium dynamics in a live fly preparation at the two-photon microscope. The neurons labeled by *R21G11* respond to all concentrations of CO_2 with the peak $\Delta F/F$ increasing from 0.5 to 1% CO_2 (Figure 2A-B, Wilcoxon signed-rank test w=66.00, p=0.0011). The peak response to 1% and 2% are not significantly different though the length of the response appears to be larger at 2% (Wilcoxon signed-rank test w=38.00, p=0.0727). We also tested responses to CO_2 in the subset of *21G11* neurons labeled by *21G11-LexA* (Figure 2C-D). To our surprise this subset responds only to 0.5% CO_2 (Wilcoxon signed-rank test w=15.00, p<0.0001). This observation suggests that within the *21G11* cluster different neurons are sensitive to different concentrations of CO_2. However, in Figure 1C we observed that when these same neurons are silenced, the behavioral response to different CO_2 concentrations does not change. Based on these findings we speculate that as soon as the activity of the neurons responsive to the lowest concentration is compromised the behavioral output to all concentrations is affected. Recordings of *23C09∩VGlut* neurons show they respond all CO_2 concentrations tested.

Though the curve of the response appears larger for lower concentrations there is no significant difference between peak amplitudes of $\Delta F/F$ of different concentrations (Figure 2E-F). In summary, both clusters respond to CO_2 stimulation at different concentrations, with each set of neurons exhibiting a different pattern of free calcium response to CO_2 stimulation.

Physiological response of *23C09∩VGlut* depends on output of *21G11-LexA*

The two sets of neurons that we identified innervate a similar region of the LH and contribute to the same behavioral response. When we silenced both clusters simultaneously we saw no additive effect, indicating they are not independent from each other to drive avoidance (Figure S2B). We therefore asked whether the two clusters are connected. To this end we used GRASP (GFP reconstitution across synaptic partners) that reveals membrane contact between two sets of neurons (34). We observe a strong signal in the LH indicating that the membranes of the two clusters contact each other (Figure 3A). To assess functional connectivity we manipulated the activity of one cluster while imaging activity on the second cluster. We silenced *21G11-LexA* neurons with the expression of *Kir2.1* using the *LexA/LexAOp* expression system and imaged *23C09∩VGlut* neurons expressing *GCaMP6.0m* with the *GAL4/UAS* system (Schematic in Figure 3B). To control for silencing we co-expressed *Kir2.1* and *GCaMP6.0m* in *21G11-LexA* neurons and confirmed that no calcium signal is observed with CO_2 stimulation (Figure S6). Upon presentation of CO_2 at the concentrations 0.5, 1 and 2%, we observed a very consistent response across trials and across concentrations in *23C09∩VGlut* neurons when *21G11-LexA* neurons are silenced (Figure 3B and C, Mann-Whitney, not significant). When we compared the peak responses of *23C09∩VGlut* while *21G11-LexA* is intact (Figure 2F) or silenced (Figure 3C), we found that there is pronounced reduction for 0.5% CO_2 responses which corresponds to the profile of *21G11-LexA* responses (Figure 3D). The results indicate that the output of *21G11-LexA* neurons contributes to *23C09∩VGlut* activity. To test this directly, we expressed

the red-shifted channelrhodopsin *Chrimson* (35) in *21G11-LexA* neurons to allow activation of *21G11-LexA* neurons with 720nm light while recording *23C09∩VGlut* calcium concentration with *GCaMP6.0m*. We observe that indeed activation of *21G11-LexA* neurons with light generates a strong calcium response in *23C09∩VGlut* neurons (Figure 3E and F). No calcium response was observed in *23C09∩VGlut* neurons when flies were not fed retinal, which is necessary for *Chrimson* function (Figure 3E and F).

We next did the converse experiments where we manipulate activity in *23C09∩VGlut* neurons and image activity in *21G11-LexA* neurons using the same tools with the expression systems reversed. Silencing *23C09∩VGlut* neurons does not change *21G11-LexA* response to CO_2 presentation (Figure 3F and G). These results indicate that *23C09∩VGlut* neurons do not output into *21G11-LexA* neurons. We then performed optogenetic activation of *23C09∩VGlut* neurons and recorded the calcium response of *21G11-LexA* neurons. We did not observe a calcium response in *21G11-LexA* neurons upon light stimulation of *23C09∩VGlut* neurons (Figure 3H). To control for activation of *23C09∩VGlut* neurons we expressed both *Chrimson* and *GCaMP6m* in these neurons and could see a response with light stimulation (Figure S7). The activation results further support the notion that *23C09∩VGlut* does not output into *21G11-LexA* neurons.

Taken together the results indicate that *21G11-LexA* neurons are presynaptic to *23C09∩VGlut* neurons. The presence of a presynaptic marker at the LH processes of *21G11-LexA* neurons is consistent with these observations (Figure 1F). Based on our findings we propose a model where CO_2 response is processed at the SIP via *21G11* output (Figure 3I). *21G11* also outputs at the LH to activate the *23C09∩VGlut* local neurons that are glutamatergic. Given that it has been proposed that glutamatergic neurons in the fly brain are inhibitory (36), we speculate that *23C09* neurons inhibit output neurons that mediate attraction.

246 ***21G11* and *23C09∩VGlut* neurons are selectively involved in processing**
247 **CO_2 avoidance**

248 We then asked if the circuit we identified at the LH is involved in the response to
249 other odors. It could be central to all odor responses or perhaps be involved only
250 in the aversive responses or even selectively involved in the CO_2 response. To
251 answer this question we first measured the calcium responses to different odors
252 (Figure 4 A-D). To test attractive odor responses we used farnesol, an attractant
253 present in the rind of ripe citrus and processed through a single glomerulus (37),
254 and apple cider vinegar, a complex attractive stimulus (38). While apple cider
255 vinegar elicits a small response in both sets of neurons, farnesol does not elicit a
256 response in either set of neurons (Figure 4A-D). To test aversive responses we
257 used benzaldehyde that smells of bitter almond and acetic acid that elicits the
258 acid sensing response in the antennal lobe (22). *21G11* neurons respond to both
259 acetic acid and benzaldehyde (Figure 4A and B). *23C09* neurons respond only to
260 benzaldehyde in an atypical fashion (Figure 4C-D). The rise in calcium
261 concentration happens a few seconds after stimulus presentation. Though the
262 peak ΔF/F in all these responses is low, the physiological response is broad and
263 includes responses to aversive and attractive odors. How do these physiological
264 responses translate into a behavioral response? To address this question we
265 tested the requirement of activity in *23C09∩VGlut* or *21G11-GAL4* (broader
266 expression than *21G11-LexA*) neurons for the behavioral response to other
267 odors. Similarly to what we did in the screen, we tested the flies using a T-maze.
268 Also following the screen conditions, we silenced the neurons with *Kir2.1* only in
269 the adult stage. We allowed the flies to choose between air and either farnesol,
270 apple cider vinegar, acetic acid or benzaldehyde at 1/1000 dilution. It was
271 reported that there is a non-olfactory component to benzaldehyde avoidance at
272 1/100 dilution. We confirmed that we are not including a non-olfactory component
273 in our experiment by testing the response of flies without olfactory organs to our
274 working dilution of benzaldehyde (Figure S8). We observe that activity in *23C09*
275 *∩VGlut* or *21G11-GAL4* neurons is not required either for attraction to farnesol
276 or apple cider vinegar indicating that activity in these LH neurons is not involved

in general odor responses (Figure 4E). Silencing *23C09∩VGlut* or *21G11-GAL4* neurons also does not affect avoidance to benzaldehyde and acetic acid (Figure 4F). Interestingly, though the arborization at the LH of the acid sensing projection neurons is very similar to the arborization of the V-glomerulus projection neurons (39), it appears that different LH neurons process these responses. The results indicate that activity in *21G11* and *23C09∩VGlut* neurons is selectively required for the response to CO_2.

DISCUSSION

In this study we used a behavioral readout to directly address the role of the LH in olfactory responses. We showed that the activity of two clusters of LH neurons is required for *D. melanogaster* innate avoidance of CO_2. Furthermore, because we have not found a correlation between the activity of these LH neurons and the behavioral responses to other general odors, we conclude that the activity of *21G11 and 23C09∩VGlut* neurons is specifically required for responses to CO_2. Thus, our results unravel a circuit within the LH region specific for CO_2 avoidance responses in the lower concentration range. However, the avoidance to CO_2 is not completely abolished by silencing these neurons. This could have three origins: not all cells are labeled in the identified cluster; unidentified clusters are involved; the LH has intricate connectivity and silencing of any LH neuron leads to disruption of the behavior. The latter is unlikely as we silenced and tested 32 lines labeling different LH neurons, some of them innervating very large sections of the LH and only the two lines described here consistently had an effect. Though we cannot eliminate any of the former possibilities, the lack of contact between the LH neurons we identified and the V-glomerulus projection neurons that carry CO_2 stimulus information argues for the involvement of additional neurons.

Recent work indicates that MB can be involved in innate aversion and the LH is required for the execution of learned aversion (10,40–42). Hence, the roles of the

two centers are not as segregated as previously thought and they must be connected to coordinate the innate and the learned responses. The *21G11* output neurons we identified connect to the superior intermediate protocerebrum. It is an area highly innervated by MB output neuron terminals (MBONs) suggesting a location for integration of LH and MB output (43,44). At the other extremity of *21G11* neurons, we showed that they output within the LH to the *23C09 ∩ VGlut* neurons. Since these are glutamatergic neurons and glutamatergic signaling in the brain can be inhibitory we speculate that activation of *21G11* and *23C09 ∩ VGlut* leads to inhibition of LH output neurons that mediate attraction.

A vast search has identified compounds that either increase or decrease the activity of the CO_2 receptors (45). It was revealed that odors increasing receptor activity generate avoidance responses and odors decreasing receptor activity generate attraction responses indicating that the CO_2 receptor pathway has a strong weight in establishing odor valence (46). Further work should elucidate how the LH neurons identified here contribute to these responses.

In summary, we demonstrated a role of the LH in an innate behavioral response. The neurons we identified appear to be involved in suppression of attraction at the LH. Moving forward, it will be interesting to explore whether a similar organization at the LH is used to generate responses to other odors and how the response is coordinated with the MB.

ACKNOWLEDGEMENTS

We thank Eugenia Chiappe, Susana Lima, Marta Moita and members of the Vasconcelos Laboratory for discussion and comments on the manuscript. Barry Dickson provided fly stock and Gerald M. Rubin provided a promoter plasmid. We would like to thank the Fly and Molecular platforms of Champalimaud Centre for the Unknown (CCU) for generating the transgenic flies and scientific hardware and software platforms of CCU for support with the optogenetic activation

experiments. This work was supported by Fundação Champalimaud, a grant from Fundação para Ciência e tecnologia (FCT) PTDC/BIA-BCM/104898/2008, FCT fellowship SFRH/BDP/77360/2011 to N.V.

AUTHOR CONTRIBUTION

N.V. and M.L.V. conceived and designed the project. M.G. performed the behavioral screen. N.V. performed all other experiments with the technical assistance of S.D. M.L.V. provided guidance and wrote the paper with N.V.

DECLARATION OF INTEREST

The authors declare no competing interests.

REFERENCES

1. Vosshall LB, Stocker RF. Molecular architecture of smell and taste in Drosophila. Annu Rev Neurosci [Internet]. 2007 Jan [cited 2011 Jul 18];30:505–33. Available from: http://www.ncbi.nlm.nih.gov/pubmed/17506643
2. Masse NY, Turner GC, Jefferis GSXE. Olfactory Information Processing in Drosophila. Curr Biol [Internet]. Elsevier Ltd; 2009;19(16):R700–13. Available from: http://dx.doi.org/10.1016/j.cub.2009.06.026
3. Wong AM, Wang JW, Axel R. Spatial representation of the glomerular map in the Drosophila protocerebrum. Cell [Internet]. 2002 Apr 19;109(2):229–41. Available from: http://www.ncbi.nlm.nih.gov/pubmed/12007409
4. Marin EC, Jefferis GSXE, Komiyama T, Zhu H, Luo L. Representation of the glomerular olfactory map in the Drosophila brain. Cell. 2002;109:243–55.
5. Keene AC, Waddell S. Drosophila olfactory memory: single genes to complex neural circuits. Nat Rev Neurosci [Internet]. 2007;8(5):341–54. Available from: http://www.nature.com/doifinder/10.1038/nrn2098
6. Heimbeck G, Bugnon V, Gendre N, Keller A, Stocker RF. A central neural

circuit for experience-independent olfactory and courtship behavior in Drosophila melanogaster. Proc Natl Acad Sci U S A. 2001;98:15336–41.

7. Parnas M, Lin AC, Huetteroth W, Miesenbo G, Miesenb??ck G. Odor Discrimination in Drosophila: From Neural Population Codes to Behavior. Neuron. 2013;79(5):932–44.

8. Datta SR, Vasconcelos ML, Ruta V, Luo S, Wong A, Demir E, et al. The Drosophila pheromone cVA activates a sexually dimorphic neural circuit. Nature [Internet]. 2008 Mar;452(7186):473–7. Available from: http://www.ncbi.nlm.nih.gov/pubmed/18305480

9. Lin H-H, Chu L-A, Fu T-F, Dickson BJ, Chiang A-S. Parallel neural pathways mediate CO2 avoidance responses in Drosophila. Science [Internet]. 2013 Jun 14 [cited 2014 Mar 25];340(6138):1338–41. Available from: http://www.ncbi.nlm.nih.gov/pubmed/23766327

10. Bräcker LB, Siju KP, Varela N, Aso Y, Zhang M, Hein I, et al. Essential role of the mushroom body in context-dependent CO_2 avoidance in Drosophila. Curr Biol [Internet]. 2013 Jul 8 [cited 2014 Mar 26];23(13):1228–34. Available from: http://www.ncbi.nlm.nih.gov/pubmed/23770186

11. Caron SJC, Ruta V, Abbott LF, Axel R. Random convergence of olfactory inputs in the Drosophila mushroom body. Nature [Internet]. Nature Publishing Group; 2013 May 2 [cited 2014 Jul 20];497(7447):113–7. Available from: http://www.ncbi.nlm.nih.gov/pubmed/23615618

12. Jefferis GSXE, Potter CJ, Chan AM, Marin EC, Rohlfing T, Maurer CR, et al. Comprehensive Maps of Drosophila Higher Olfactory Centers: Spatially Segregated Fruit and Pheromone Representation. Cell. 2007;128:1187–203.

13. Strutz A, Soelter J, Baschwitz A, Farhan A, Grabe V, Rybak J, et al. Decoding odor quality and intensity in the Drosophila brain. Elife. 2014;3:e04147.

14. Ruta V, Datta SR, Vasconcelos ML, Freeland J, Looger LL, Axel R. A dimorphic pheromone circuit in Drosophila from sensory input to descending output. Nature [Internet]. Nature Publishing Group; 2010 Dec 2

[cited 2011 Jun 15];468(7324):686–90. Available from: http://www.ncbi.nlm.nih.gov/pubmed/21124455

15. Kohl J, Ostrovsky AD, Frechter S, Jefferis GSXE. A bidirectional circuit switch reroutes pheromone signals in male and female brains. Cell [Internet]. The Authors; 2013 Dec 19 [cited 2014 Mar 26];155(7):1610–23. Available from: http://www.pubmedcentral.nih.gov/articlerender.fcgi?artid=3898676&tool=pmcentrez&rendertype=abstract

16. Luo SX, Axel R, Abbott LF. Generating sparse and selective third-order responses in the olfactory system of the fly. Proc Natl Acad Sci U S A [Internet]. 2010 Jun 8 [cited 2014 Oct 3];107(23):10713–8. Available from: http://www.pubmedcentral.nih.gov/articlerender.fcgi?artid=2890779&tool=pmcentrez&rendertype=abstract

17. Fişek M, Wilson RI. Stereotyped connectivity and computations in higher-order olfactory neurons. Nat Neurosci [Internet]. 2014 Feb [cited 2014 Mar 22];17(2):280–8. Available from: http://www.ncbi.nlm.nih.gov/pubmed/24362761

18. Kwon JY, Dahanukar A, Weiss LA, Carlson JR. The molecular basis of CO2 reception in Drosophila. Proc Natl Acad Sci U S A [Internet]. 2007 Feb 27;104(9):3574–8. Available from: http://www.ncbi.nlm.nih.gov/pubmed/17360684

19. Jones WD, Cayirlioglu P, Kadow IG, Vosshall LB. Two chemosensory receptors together mediate carbon dioxide detection in Drosophila. Nature [Internet]. 2007 Jan;445(7123):86–90. Available from: http://www.ncbi.nlm.nih.gov/pubmed/17167414

20. Suh GSB, Wong AM, Hergarden AC, Wang JW, Simon AF, Benzer S, et al. A single population of olfactory sensory neurons mediates an innate avoidance behaviour. Dros Nat. 2004;431:854–9.

21. Suh GSB, Ben-Tabou de Leon S, Tanimoto H, Fiala A, Benzer S, Anderson DJ. Light activation of an innate olfactory avoidance response in Drosophila. Curr Biol [Internet]. 2007 May 15 [cited 2014 Mar

20];17(10):905–8. Available from: http://www.ncbi.nlm.nih.gov/pubmed/17493811

22. Ai M, Min S, Grosjean Y, Leblanc C, Bell R, Benton R, et al. Acid sensing by the Drosophila olfactory system. Nature [Internet]. 2010 Dec 2 [cited 2014 Jul 24];468(7324):691–5. Available from: http://www.pubmedcentral.nih.gov/articlerender.fcgi?artid=3105465&tool=pmcentrez&rendertype=abstract

23. Breugel F Van, Huda A, Dickinson MH. Drosophila have distinct activity-gated pathways that mediate attraction and aversion to CO 2. 2017;1–8.

24. Pfeiffer BD, Jenett A, Hammonds AS, Ngo T-TB, Misra S, Murphy C, et al. Tools for neuroanatomy and neurogenetics in Drosophila. Proc Natl Acad Sci U S A [Internet]. 2008 Jul;105(28):9715–20. Available from: http://www.pubmedcentral.nih.gov/articlerender.fcgi?artid=2447866&tool=pmcentrez&rendertype=abstract

25. Jenett A, Rubin GM, Ngo T-TTB, Shepherd D, Murphy C, Dionne H, et al. A GAL4-driver line resource for Drosophila neurobiology. Cell Rep [Internet]. The Authors; 2012 Oct 25 [cited 2014 Jul 15];2(4):991–1001. Available from: http://www.pubmedcentral.nih.gov/articlerender.fcgi?artid=3515021&tool=pmcentrez&rendertype=abstract

26. Baines RA, Uhler JP, Thompson A, Sweeney ST, Bate M. Altered Electrical Properties in Drosophila neurons developing without synaptic transmission. J Neurosci [Internet]. 2001 Mar 1 [cited 2014 Oct 16];21(5):1523–31. Available from: http://www.jneurosci.org/content/21/5/1523.short

27. McGuire SE, Mao Z, Davis RL. Spatiotemporal gene expression targeting with the TARGET and gene-switch systems in Drosophila. Sci STKE [Internet]. 2004 Feb 17 [cited 2014 Mar 21];2004(220):pl6. Available from: http://www.ncbi.nlm.nih.gov/pubmed/14970377

28. Tanaka NK, Awasaki T, Shimada T, Ito K. Integration of chemosensory pathways in the Drosophila second-order olfactory centers. Curr Biol

463 [Internet]. 2004 Mar 23;14(6):449–57. Available from:
464 http://www.ncbi.nlm.nih.gov/pubmed/15043809
465 29. Luan H, Peabody NCN, Vinson CRC, White BBH. Refined spatial
466 manipulation of neuronal function by combinatorial restriction of transgene
467 expression. Neuron [Internet]. 2006 [cited 2014 Oct 17];52(3):425–36.
468 Available from:
469 http://www.sciencedirect.com/science/article/pii/S089662730600674X
470 30. Diao FF, Ironfield H, Luan H, Diao FF, Shropshire WC, Ewer J, et al. Plug-
471 and-Play Genetic Access to Drosophila Cell Types using Exchangeable
472 Exon Cassettes. Cell Rep [Internet]. The Authors; 2015;10(8):1410–21.
473 Available from:
474 http://www.sciencedirect.com/science/article/pii/S2211124715001011
475 31. Wang J, Ma X, Yang JS, Zheng X, Zugates CT, Lee CHJ, et al.
476 Transmembrane/juxtamembrane domain-dependent Dscam distribution
477 and function during mushroom body neuronal morphogenesis. Neuron.
478 2004;43(5):663–72.
479 32. Robinson IM, Ranjan R, Schwarz TL. Synaptotagmins I and IV promote
480 transmitter release independently of Ca(2+) binding in the C(2)A domain.
481 Nature [Internet]. 2002 Jul 18;418(6895):336–40. Available from:
482 http://www.ncbi.nlm.nih.gov/pubmed/12110845
483 33. Chen T-W, Wardill TJ, Sun Y, Pulver SR, Renninger SL, Baohan A, et al.
484 Ultrasensitive fluorescent proteins for imaging neuronal activity. Nature
485 [Internet]. 2013 Jul 18 [cited 2014 Mar 19];499(7458):295–300. Available
486 from:
487 http://www.pubmedcentral.nih.gov/articlerender.fcgi?artid=3777791&tool=p
488 mcentrez&rendertype=abstract
489 34. Gordon MD, Scott K. Motor control in a Drosophila taste circuit. Neuron
490 [Internet]. Elsevier Ltd; 2009 Feb;61(3):373–84. Available from:
491 http://www.pubmedcentral.nih.gov/articlerender.fcgi?artid=2650400&tool=p
492 mcentrez&rendertype=abstract
493 35. Klapoetke NC, Murata Y, Kim SS, Pulver SR, Birdsey-Benson A, Cho YK,

et al. Independent optical excitation of distinct neural populations. Nat Methods [Internet]. Nature Publishing Group; 2014 Mar [cited 2014 Apr 28];11(3):338–46. Available from: http://www.ncbi.nlm.nih.gov/pubmed/24509633

36. Liu WW, Wilson RI. Glutamate is an inhibitory neurotransmitter in the Drosophila olfactory system. 2013;2013.

37. Ronderos DS, Lin C, Potter CJ, Smith DP. Farnesol-Detecting Olfactory Neurons in Drosophila. 2014;34(11):3959–68.

38. Semmelhack JL, Wang JW. Select Drosophila glomeruli mediate innate olfactory attraction and aversion. Nature [Internet]. 2009 May 14 [cited 2014 Jul 30];459(7244):218–23. Available from: http://www.pubmedcentral.nih.gov/articlerender.fcgi?artid=2702439&tool=pmcentrez&rendertype=abstract

39. Min S, Ai M, Shin S a, Suh GSB. Dedicated olfactory neurons mediating attraction behavior to ammonia and amines in Drosophila. Proc Natl Acad Sci U S A [Internet]. 2013 Apr 2 [cited 2014 Sep 10];110(14):E1321-9. Available from: http://www.pubmedcentral.nih.gov/articlerender.fcgi?artid=3619346&tool=pmcentrez&rendertype=abstract

40. Lewis LPC, Siju KP, Aso Y, Friedrich AB, Bulteel AJB, Rubin GM, et al. A Higher Brain Circuit for Immediate Integration of Conflicting Sensory Information in Drosophila. Curr Biol [Internet]. Elsevier Ltd; 2015 Aug 31;25(17):2203–14. Available from: http://dx.doi.org/10.1016/j.cub.2015.07.015

41. Dolan M, Belliart-Guérin G, Bates AS, Aso Y, Frechter S, Roberts RJV, et al. Communication from learned to innate olfactory processing centers is required for memory retrieval in Drosophila. bioRxiv. 2017;

42. Séjourné J, Plaçais P-Y, Aso Y, Siwanowicz I, Trannoy S, Thoma V, et al. Mushroom body efferent neurons responsible for aversive olfactory memory retrieval in Drosophila. Nat Neurosci [Internet]. Nature Publishing

525 Group; 2011 Jul [cited 2014 Mar 19];14(7):903–10. Available from:
526 http://www.ncbi.nlm.nih.gov/pubmed/21685917
527 43. Aso Y, Sitaraman D, Ichinose T, Kaun KR, Vogt K, Belliart-Guérin G, et al.
528 Mushroom body output neurons encode valence and guide memory-based
529 action selection in Drosophila. Elife [Internet]. 2014;3(3):1–42.
530 Available from: http://elifesciences.org/lookup/doi/10.7554/eLife.04580
531 44. Aso Y, Hattori D, Yu Y, Johnston RM, Nirmala a, Ngo T, et al. The
532 neuronal architecture of the mushroom body provides a logic for
533 associative learning. Elife. 2014;1–47.
534 45. Tauxe GM, Macwilliam D, Boyle SM, Guda T, Ray A. Targeting a dual
535 detector of skin and CO2 to modify mosquito host seeking. Cell [Internet].
536 Elsevier; 2013;155(6):1365–79. Available from:
537 http://dx.doi.org/10.1016/j.cell.2013.11.013
538 46. MacWilliam D, Kowalewski J, Kumar A, Pontrello C, Ray A. Signaling
539 Mode of the Broad-Spectrum Conserved CO2Receptor Is One of the
540 Important Determinants of Odor Valence in Drosophila. Neuron [Internet].
541 Elsevier Inc.; 2018;97(5):1153–1167.e4. Available from:
542 https://doi.org/10.1016/j.neuron.2018.01.028
543 47. Lee T, Luo L. Mosaic analysis with a repressible cell marker for studies of
544 gene function in neuronal morphogenesis. Neuron [Internet].
545 1999;22(3):451–61. Available from:
546 http://www.ncbi.nlm.nih.gov/pubmed/10197526
547 48. Pfeiffer BD, Ngo T-TB, Hibbard KL, Murphy C, Jenett A, Truman JW, et al.
548 Refinement of Tools for Targeted Gene Expression in Drosophila. Genetics
549 [Internet]. 2010 Aug [cited 2010 Sep 6];16. Available from:
550 http://www.ncbi.nlm.nih.gov/pubmed/20697123
551 49. Feng K, Palfreyman MT, Häsemeyer M, Talsma A, Dickson BJ, Feng K, et
552 al. Ascending SAG Neurons Control Sexual Receptivity of Drosophila
553 Females. Neuron [Internet]. 2014 Jul 2 [cited 2014 Jul 10];83(1):135–48.
554 Available from: http://www.ncbi.nlm.nih.gov/pubmed/24991958
555 50. Fosque BF, Sun Y, Dana H, Yang C, Ohyama T, Tadross MR, et al.

Labeling of active neural circuits in vivo with designed calcium integrators. 2015;347(6223).

51. Nern A, Pfeiffer BD, Rubin GM. Optimized tools for multicolor stochastic labeling reveal diverse stereotyped cell arrangements in the fly visual system. Proc Natl Acad Sci [Internet]. 2015;112(22):E2967–76. Available from: http://www.pnas.org/lookup/doi/10.1073/pnas.1506763112

52. Lai S-L, Lee T. Genetic mosaic with dual binary transcriptional systems in Drosophila. Nat Neurosci [Internet]. 2006 May;9(5):703–9. Available from: http://www.ncbi.nlm.nih.gov/pubmed/16582903

53. Tully T, Quinn WG. Classical conditioning and retention in normal and mutant Drosophila melanogaster. J Comp Physiol A [Internet]. 1985;157(2):263–77. Available from: https://www.scopus.com/inward/record.uri?eid=2-s2.0-0022119763&partnerID=40&md5=ce08627d42785c31cec54558786f6954

54. Chiappe ME, Jayaraman V. Genetically Encoded Functional Indicators [Internet]. Martin J-R, editor. Totowa, NJ: Humana Press; 2012 [cited 2014 Mar 26]. 83-101 p. (Neuromethods; vol. 72). Available from: http://link.springer.com/10.1007/978-1-62703-014-4

MATERIALS AND METHODS

Contact for Reagent and Resource Sharing

Further information and requests for resources and reagents should be directed to and will be fulfilled by the lead contact Maria Luísa Vasconcelos (maria.vasconcelos@neuro.fchampalimaud.org).

Experimental Model and Subject Details

Flies were maintained on standard cornmeal-agar medium at 18ºC or 25ºC and 70% relative humidity under a 12h light/dark cycle. Fly strains used were as follows: *UAS-Kir2.1* (26); *tub-GAL80^{TS}* (27); *UAS-Chrimson* (35); *UAS-GCaMP6.0m* (33); *UAS-Dscam17.1-GFP* (31); *UAS-syt-HA* (32); *UAS-CD4-*

587 *GFP$_{1-10}$* (34); *UAS-CD8-GFP* (47); *UAS-VGlutDBD* (30); *UAS-myr-tdTomato*(48);
588 *LexAop-Kir2.1 (provived by Barry Dickson)* (49); *LexAop-Chrimson* (50); *LexAop-*
589 *GCaMP6.0m* (33); *LexAop-syt-HA* (51); *LexAop-CD4-GFP$_{11}$* (34); *LexAop-*
590 *mCD2-GFP*(52). We used the following *GAL4* lines: *R21G11*; *R23C09*; *R84A06*;
591 *R65D12*; *R19B07*; *R13A11*; *R30A10*; *R37G11*; *R33E01*; *R93D02*; *R93D05*;
592 *R41F11*; *R85C07*; *R64B02*; *R36E10*; *R30H02*; *R25B07*; *R36G09*; *R23F06*;
593 *R54G12*; *R16C09*; *R13A07*; *R22B02*; *R29F04*; *R16C06*; *R82E01*; *R25A01*;
594 *R84G12*; *R25G10*; *R26C12*; *R20C09*; *R20B0* from the Janelia farm collection
595 (24,25).
596
597 **Genotypes per Figure**
598
599 **Figure 1**
600 Panel A
601 *w^{1118};UAS-Kir2.1,tub-Gal80^{TS};+*
602 *w^{1118};UAS-Kir2.1,tub-Gal80^{TS};21G11-GAL4*
603 *w^{1118};UAS-Kir2.1,tub-Gal80^{TS};23C09-GAL4*
604
605 Panel B
606 *w^{1118};LexAop-Kir2.1;+*
607 *w^{1118}; ;LexAop-Kir2.1;21G11-LexA*
608
609 Panel C
610 *w^{1118};UAS-Kir2.1,tub-Gal80^{TS};+*
611 *w^{1118};UAS-Kir2.1,tub-Gal80^{TS};23C09-AD/UAS-VGlut-DBD*
612
613 Panel D
614 *w^{1118};+;21G11-GAL4/UAS-mCD8-GFP*
615 *w^{1118};LexAop-mCD2-GFP/+;21G11-LexA/+*
616
617 Panel E

618 *w^{1118};+;23C09-GAL4/UAS-mCD8-GFP/+*

619 *w^{1118};23C09-AD/UAS-VGlut-DBD;UAS-mCD8-GFP/+*

620

621 Panel F and G

622 *w^{1118};UAS-Dscam-17.1-GFP;21G11-GAL4*

623 *w^{1118};UAS-syt-HA;21G11-GAL4*

624

625 Panel H

626 *w^{1118};21G11-LexA/LexAop-CD2-GFP;UAS-myr-tdTomato/53A05-GAL4*

627 *w^{1118}; 21G11-LexA/ LexAop-CD2-GFP;UAS-myr-tdTomato /41C05-GAL4*

628

629 Panel I

630 *w^{1118}; 23C09-AD/UAS-VGlut-DBD/+;UAS-mCD8-GFP/53A05-GAL4*

631 *w^{1118}; 23C09-AD/UAS-VGlut-DBD/+;UAS-mCD8-GFP/41C05-GAL4*

632

633

634 **Figure 2**

635 Panel A and B

636 *w^{1118};21G11-GAL4;UAS-GCaMP6.0m*

637

638 Panel C and D

639 *w^{1118};21G11-LexA;21G11-LexA/LexAop-GCaMP6.0m*

640

641 Panel E and F

642 *w^{1118};23C09-AD/UAS-VGlut-DBD;UASGCaMP6.0m*

643

644

645 **Figure 3**

646 Panel A

647 *w^{1118};LexAop-CD4-GFP$_{11}$/21G11-LexA;UAS-mCD4-GFP$_{1-10}$/23C09-GAL4*

648

649 Panel B, C and D

650 *w^{1118};21G11-LexA,LexAop-Kir2.1/23C09-AD,UAS-VGlut-DBD;21G11-LexA/UAS-*

651 *GCaMP6.0m*

652

653 Panel E and F

654 *w^{1118};21G11-LexA,LexAop-Chrimson/23C09-AD,UAS-VGlut-DBD;21G11-*

655 *LexA/UASGCaMP6.0m*

656

657 Panel G and H

658 *w^{1118};21G11-LexA/23C09-AD,UAS-VGlut-DBD;21G11-LexA,LexAop-*

659 *GCaMP6.0m/UAS-Kir2.1*

660

661 Panel I

662 *w^{1118};21G11-LexA/23C09-AD,UAS-VGlut-DBD;21G11-LexA,LexAop-*

663 *GCaMP6.0m/UAS-Chrimson*

664

665

666 **Figure 4**

667 Panel A and B

668 *w^{1118};21G11-LexA;21G11-LexA/LexAop-GCaMP6.0m*

669

670 Panel C and D

671 *w^{1118};23C09-AD/UAS-VGlut-DBD;UASGCaMP6.0m*

672

673 Panel E and F

674 *w^{1118};UAS-Kir2.1,tub-Gal80^{TS};+*

675 *w^{1118};UAS-Kir2.1,tub-Gal80^{TS};21G11-GAL4*

676 *w^{1118};UAS-Kir2.1,tub-Gal80^{TS};23C09-GAL4*

677

678 **Figure Supp 1**

679 Panel A

680 *w^{1118};UAS-Kir2.1,tub-Gal80^{TS};84A06-GAL4*
681 *w^{1118};UAS-Kir2.1,tub-Gal80^{TS};65D12-GAL4*
682 *w^{1118};UAS-Kir2.1,tub-Gal80^{TS};21G11-GAL4*
683 *w^{1118};UAS-Kir2.1,tub-Gal80^{TS};23C09-GAL4*
684 *w^{1118};UAS-Kir2.1,tub-Gal80^{TS};19B07-GAL4*
685 *w^{1118};UAS-Kir2.1,tub-Gal80^{TS};13A11-GAL4*
686 *w^{1118};UAS-Kir2.1,tub-Gal80^{TS};30A10-GAL4*
687 *w^{1118};UAS-Kir2.1,tub-Gal80^{TS};37G11-GAL4*
688 *w^{1118};UAS-Kir2.1,tub-Gal80^{TS};33E01-GAL4*
689 *w^{1118};UAS-Kir2.1,tub-Gal80^{TS};93D02-GAL4*
690 *w^{1118};UAS-Kir2.1,tub-Gal80^{TS};93D05-GAL4*
691 *w^{1118};UAS-Kir2.1,tub-Gal80^{TS};41F11-GAL4*
692 *w^{1118};UAS-Kir2.1,tub-Gal80^{TS};85C07-GAL4*
693 *w^{1118};UAS-Kir2.1,tub-Gal80^{TS};64B02-GAL4*
694 *w^{1118};UAS-Kir2.1,tub-Gal80^{TS};36E10-GAL4*
695 *w^{1118};UAS-Kir2.1,tub-Gal80^{TS};30H02-GAL4*
696 *w^{1118};UAS-Kir2.1,tub-Gal80^{TS};25B07-GAL4*
697 *w^{1118};UAS-Kir2.1,tub-Gal80^{TS};36G09-GAL4*
698 *w^{1118};UAS-Kir2.1,tub-Gal80^{TS};23F06 GAL4*
699 *w^{1118};UAS-Kir2.1,tub-Gal80^{TS};54G12-GAL4*
700 *w^{1118};UAS-Kir2.1,tub-Gal80^{TS};16C09-GAL4*
701 *w^{1118};UAS-Kir2.1,tub-Gal80^{TS};13A07-GAL4*
702 *w^{1118};UAS-Kir2.1,tub-Gal80^{TS};22B02-GAL4*
703 *w^{1118};UAS-Kir2.1,tub-Gal80^{TS};29F04-GAL4*
704 *w^{1118};UAS-Kir2.1,tub-Gal80^{TS};16C06-GAL4*
705 *w^{1118};UAS-Kir2.1,tub-Gal80^{TS};82E01-GAL4*
706 *w^{1118};UAS-Kir2.1,tub-Gal80^{TS};25A01-GAL4*
707 *w^{1118};UAS-Kir2.1,tub-Gal80^{TS};84G12-GAL4*
708 *w^{1118};UAS-Kir2.1,tub-Gal80^{TS};25G10-GAL4*
709 *w^{1118};UAS-Kir2.1,tub-Gal80^{TS};26C12-GAL4*
710 *w^{1118};UAS-Kir2.1,tub-Gal80^{TS};20C09-GAL4*

711 *w^{1118};UAS-Kir2.1,tub-$Gal80^{TS}$;20B07-GAL4*

712

713 Panel B

714 *w^{1118};UAS-Kir2.1,tub-$Gal80^{TS}$;65D12-GAL4*

715 *w^{1118};UAS-Kir2.1,tub-$Gal80^{TS}$;21G11-GAL4*

716 *w^{1118};UAS-Kir2.1,tub-$Gal80^{TS}$;23C09-GAL4*

717 *w^{1118};UAS-Kir2.1,tub-$Gal80^{TS}$;13A11-GAL4*

718 *w^{1118};UAS-Kir2.1,tub-$Gal80^{TS}$;33E01-GAL4*

719 *w^{1118};UAS-Kir2.1,tub-$Gal80^{TS}$;85C07-GAL4*

720 *w^{1118};UAS-Kir2.1,tub-$Gal80^{TS}$;36G09-GAL4*

721 *w^{1118};UAS-Kir2.1,tub-$Gal80^{TS}$;16C09-GAL4*

722

723 **Figure Supp 2**

724 Panel A and B

725 *w^{1118};UAS-Kir2.1,tub-$Gal80^{TS}$;+*

726 *w^{1118};UAS-Kir2.1,tub-$Gal80^{TS}$;21G11-GAL4*

727 *w^{1118};UAS-Kir2.1,tub-$Gal80^{TS}$;23C09-GAL4*

728

729 **Figure Supp 3**

730

731 *w^{1118};LexAop-mCD2-GFP/+;21G11-LexA/+*

732 *w^{1118};23C09-AD/UAS-VGlut-DBD;UAS-mCD8-GFP/+*

733

734

735 **Figure Supp 4**

736 *w^{1118};UAS-myR-TdTomato/LexAop-mCD2-GFP;21G11-LexA/21G11-GAL4*

737

738 **Figure Supp 5**

739 *w^{1118};UAS-syt-HA;21G11-LexA*

740

741 **Figure Supp 6**

Panel A and B

w^{1118};21G11-LexA,LexAop-Kir2.1/21G11-LexA/UAS-GCaMP6.0m

Panel C and D

w^{1118};23C09-AD/UAS-VGlut-DBD;UASGCaMP6.0m/UAS-Kir2.1

Figure Supp 7

Panel A and B

w^{1118};21G11-LexA,LexAop-Chrimson/21G11-LexA/UAS-GCaMP6.0m

Panel C and D

w^{1118};23C09-AD/UAS-VGlut-DBD;UASGCaMP6.0m/UAS-Chrimson

Figure Supp 8

Panel A

w^{1118};UAS-Kir2.1,tub-Gal80^{TS};+

Method Details

Generating transgenic flies

For the establishment of the *21G11LexA* line we used the Gateway System. The *LexA* vector used was purchased from Addgene (Plasmid #26230). We carried out a genomic PCR with the primers (5' to 3') F-GGGGACAAGTTTGTACAAAAAAGCAGGCTTCGCGCAGCACGTGAAGAACAAGGC and R-GGGGACCACTTTGTACAAGAAAGCTGGGTCATGGCAACGTACTTCCAGTCCTCT. The fragment was inserted in a pDONR221 vector and then recombined

into the pBPnlsLexA::p65Uw vector (Addgene, Plasmid #26230). To construct the *23C09AD* line we use the fragment in a pDON that was kindly provided by the Rubin Lab. We recombined it as described above.

Immunostaining

Adult fly brains were dissected, fixed and stained using standard protocols. Briefly, tissue was dissected in phosphate-buffered saline (PBS), fixed in 4% PFA in PBL (PBS and 0.12M Lysine) for 30 min at room temperature, washed 3x for 5 min in PBT (PBS and 0.5% Triton X-100) and blocked for 15 minutes in 10% normal goat serum in PBT (Sigma, cat# G9023). Samples were then incubated with primary antibodies for 72h at 4ºC. After they were washed 3x for 5 min in PBT and incubated with secondary antibodies for 72h at 4ºC. Finally the samples were washed 3x for 5 min in PBT and mounted in Vectashield (Vector laboratories, cat# H-1000). As primary antibodies we used: rabbit anti-GFP (1:2000, Molecular Probes, cat# 11122), chicken anti-GFP (1:2000, Molecular Probes, cat# A10262), rabitt anti-DsRed (1:2000, Molecular Probes, cat# 710530) and mouse anti-nc82 (1:10, Developmental Studies Hybridoma Bank). The secondary antibodies used were anti-rabbit or anti-chicken IgG conjugated to Alexa 488, anti-mouse or anti-rabitt IgG conjugated to Alexa 594 and anti-mouse IgG conjugated to Alexa 405. All microscopy of immunostainings was performed with a Zeiss LSM 710 confocal microscope. Images were processed with ImageJ.

Behavioral experiments

Neuronal silencing – Flies were kept at 18ºC for 8 to 16 days. When using the *UASKir2.1,TubGAL80^{ts}*, tester flies were placed at 30ºC 24h before the experiment while control flies were always kept at 18ºC. On the day of the experiment both tester and control flies were transferred to 25ºC where we quantified their response on a T-maze (53). When using the *LexAopKir2.1* both tester and control flies were always kept at 25ºC. We quantified flies response to air, three concentrations of CO_2 (0.5%, 1% and 2%), two known attractive (apple

804 cider vinegar (ACV) and farnesol (F)) and two known repulsive compounds
805 (benzaldehyde (BZ) and acetic acid (AA)). To obtain the CO_2 concentrations we
806 mixed bottled synthetic air with bottled CO_2 (Linde). The flow rate used was of
807 0.12 l per min. All other compounds were diluted 1:1000 in paraffin oil (Sigma).
808 To test for the non-olfactory component to BZ avoidance the olfactory organs
809 were removed manually (antennae and maxillary palps) 24h before the
810 experiment. For all experiments flies were tested in groups of 20 individuals.
811 Flies were placed on the T-maze elevator and dropped to the choice area where
812 they were given 45 seconds to choose an arm. To control if the T-maze was
813 balanced, we tested flies to air on both sides. For control and tester flies, one
814 arm of the T-maze released air while the other arm released the testing
815 compound. After the experiment, flies were counted and the odor preference
816 index was calculated by subtracting the number of flies on the air side from the
817 number of flies on the other side and dividing it with the total number of flies.
818
819 Calcium imaging experiments
820 *Preparation* - For all calcium imaging experiments flies expressed the calcium
821 indicator *GCaMP6.0m*. The preparation was based on walking behavior
822 preparation (54) but without the ball. To image the lateral horn (LH) in an *in* vivo
823 preparation we glued the fly head to a microscope base (Scientifica) with bee's
824 wax (Sigma). We then opened a window that corresponded to half of the fly brain
825 and removed all fat and trachea. We made sure that both antennae were
826 untouched and healthy.
827
828 *Microscopy* - We used an Ultima two-photon laser-scanning microscope from
829 Prairie Technologies (now Bruker) and a Coherent Chameleon XR lasers. All
830 images were acquired every 0.2 ms with an Olympus BX61 microscope equipped
831 with a 40x0.8 NA objective. To measure the fluorescent intensity at the LH we
832 used ImageJ. The region of interest was delineated by hand and the result time
833 trace was used for further analysis. To calculate the normalized change in the
834 relative fluorescence intensity we used the $\Delta F/F=100(F_n-F_0)/F_0$ where F_n is the

835 *nth* frame after stimulation and F_0 is the average basal fluorescence before the
836 stimulation. Images with visible rhythmic movements of the animal were
837 discarded.
838
839 *Olfactory stimulation* – For olfactory stimulation a custom made delivery system
840 consisting of a four-way solenoid valve (Parker Hannifin) connected to a
841 peristaltic pump (Ismatec) creating a continuous airstream (1800 ml/min) that
842 was delivered to the antennae with chemically inert tubing (Ismatec). The valve
843 stimulation was commanded through the PrairieView software. For the CO_2
844 stimulation, dilutions were placed in Tedlar gas sampling bags (#24634, Sigma)
845 that were then connected to the valve. For stimulation with other compounds
846 dilutions were made in glass vials with rubber taps (Fisher). At the rubber tap we
847 inserted two venofix needles (Braun): one to connect the vial to the valve, the
848 other to connect the vial to the air in the room for air-flow in the vial. We setup the
849 system so that when a stimulus is triggered the odor dilutions replace only 50%
850 of the air-flow in order to minimize the turbulence. For this reason all dilutions
851 were prepared to double of the desired concentrations. In all experiments stimuli
852 were delivered for one second. To control for calcium changes with the air-flow,
853 all stimulations were repeated twice. In addition we performed experiments both
854 in and outside the LH, and imaged the LH in neurons with both *Kir2.1* and
855 *GCaMP6.0m*. No interference from the air-flow in the calcium response was ever
856 observed.
857
858 *Neuronal activation* – For the neuronal activation we used 8 LEDs of 720 nm
859 wavelength in a custom made ring placed beneath the stage that surrounded the
860 fly. The delivery of light to the fly was commanded through the PrairieView
861 software. The stimulus was delivered for one second at 5 Hz and 40 ms pulses.
862
863 *Neuronal silencing* – For the neuronal silencing experiments all flies expressed
864 *Kir2.1*.
865

866 **Quantification and Statistical Analysis**

867 All behavioral data was statistically analyzed by one-way analysis of variance
868 and a Sidak's multiple comparisons test. For all imaging data a Wilcoxon signed-
869 rank test comparison was performed. For all analysis and statistical tests we
870 used the GraphPad Prism Software version 6.0 (GraphPad Software).

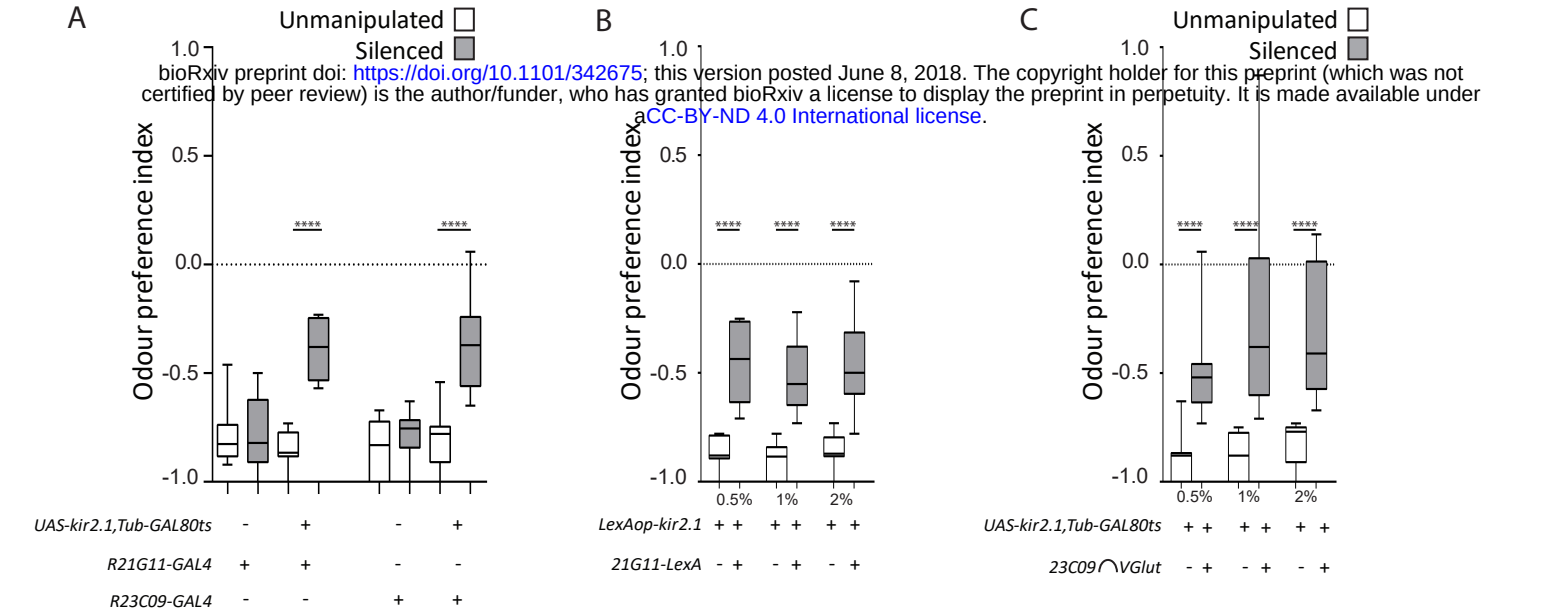

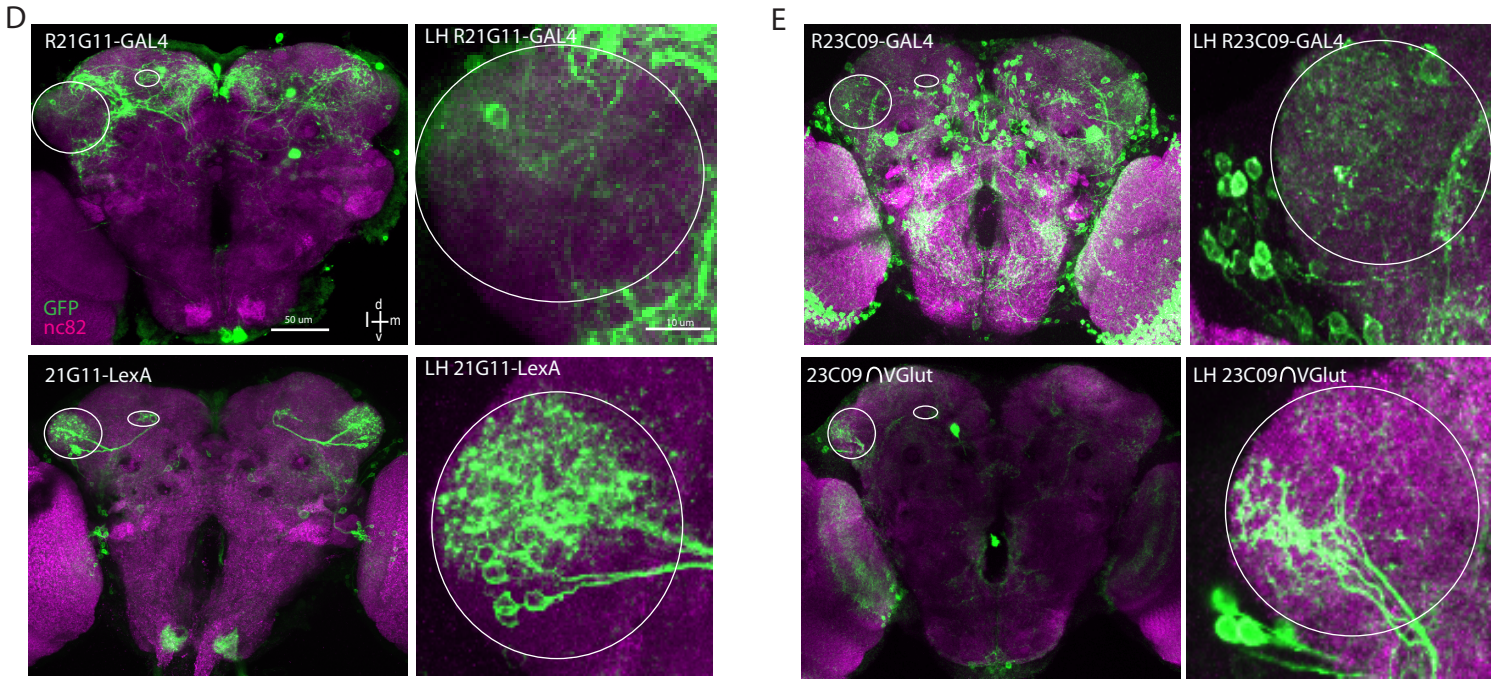

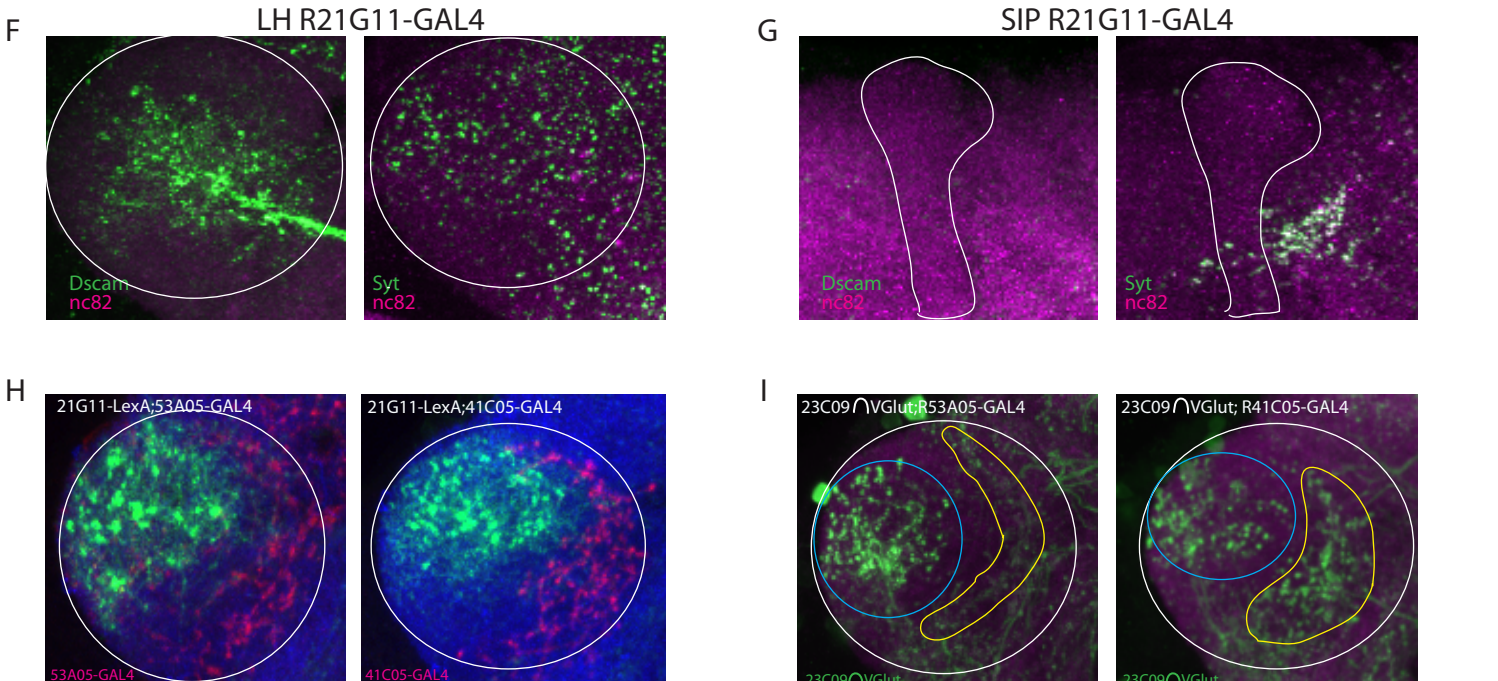

Figure 1
Activity in 21G11 and 23C09 neurons is required for behavioral response to CO2

(A) T-maze response to 1% CO2 of R21G11-GAL4 and R23C09-GAL4 flies driving UAS-Kir, TubGAL80TS expression. (A and C) White boxes, no heat induction of Kir2.1 expression ("unmanipulated", see materials and methods). Grey boxes, heat induction of Kir2.1 expression before test ("silenced"). The box represents the first and the third quartiles and the whiskers the 10th and 90th percentiles. The line across the box is the median.

(B and C) T-maze response to three CO2 concentrations - 0.5%, 1% and 2% - of the flies with 21G11-LexA driving LexAopKir2.1 expression (B) and 23C09∩VGlut driving UAS-Kir, TubGAL80TS expression (C). For 21G11-LexA driving LexAopkir2.1 expression, white boxes represent parental controls and grey boxes represent constitutive Kir expression. For 23C09∩VGlut driving UAS-Kir, TubGAL80TS expression, white boxes represent no heat induction of Kir expression and grey boxes represent heat induction of Kir expression before test. Post-hoc two-way ANOVA showed no significance when comparing among expressions for both control and test samples.

(D) Brain and lateral horn (LH) UAS-mCD8-GFP expression of R21G11-GAL4 and 21G11-LexA (green).

(E) Brain and LH UAS-mCD8-GFP expression of R23C09-GAL4 and 23C09∩VGlut (green).

(D-E) Circle highlights the LH and oval highlights the superior intermediate protocerebrum (SIP).

(F and G) Dscam 17.1-GFP and syt-HA expression in the LH and SIP of R21G11-GAL4 (green). In (F) circle highlights the LH. In (G) the vertical lobe of the mushroom body is drawn to facilitate visualization of the adjacent SIP.

(H) LH showing expression of 21G11-LexA (green) and the V-projection neuron lines R53A05-GAL4 (red) and R41C05-GAL4 (red). Circle highlights the LH.

(I) LH expression of 23C09∩Vglut (blue circles) and the V-projection neuron lines R53A05-GAL4 (yellow circle) and R41C05-GAL4 (yellow circle). White circle highlights the LH.

For all images the brain neuropil was stained with nc82 (magenta and blue). d=dorsal; l=lateral; m=medial; v=ventral.

N=9-10; ±SEM ****p<0.0001. All p values are calculated with one-way ANOVA.

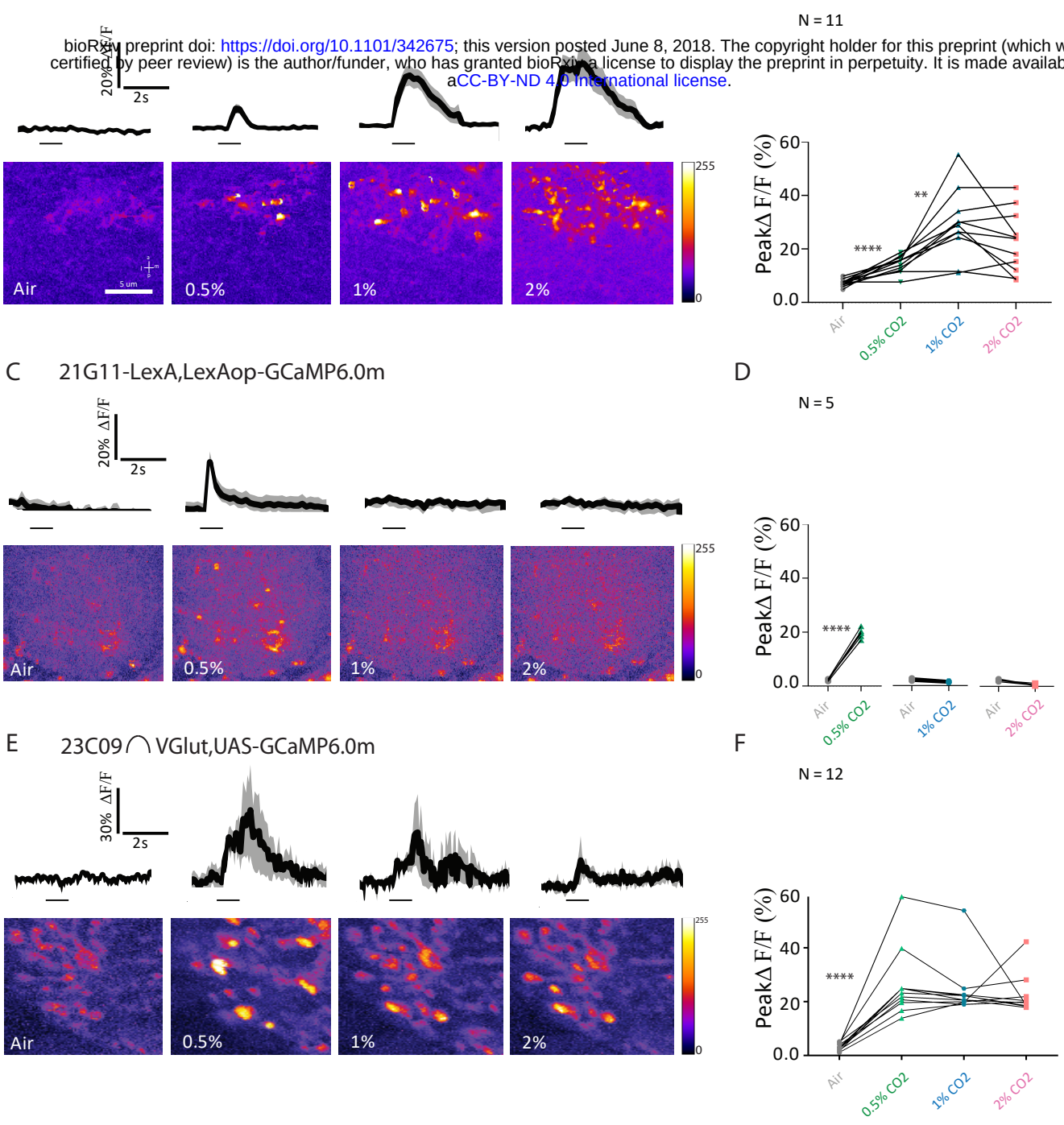

Figure 2
Physiological response to CO2 of 21G11 and 23C09 neurons

(A,C and E) LH activity of R21G11-GAL4, 21G11-LexA and 23C09∩VGlut, respectively to air, 0.5%, 1% and 2% of CO2. On top it is shown the average time course of GCaMP6.0m intensity change. The black bar indicates the time of the stimulus. The black trace represents the average while the grey shows the range of individual traces. On bottom the representative images showing the pseudo-colored response.
(B,D and F) Peak GCaMP6.0m intensity change after stimulation with air, 0.5%, 1% and 2% of CO2.
a=anterior; l=lateral; m=medial; p=posterior. Error bars indicate ±SEM, **p<0.01,***p<0.001, ****p<0.0001. All p values are calculated with Wilcoxon signed-rank test.

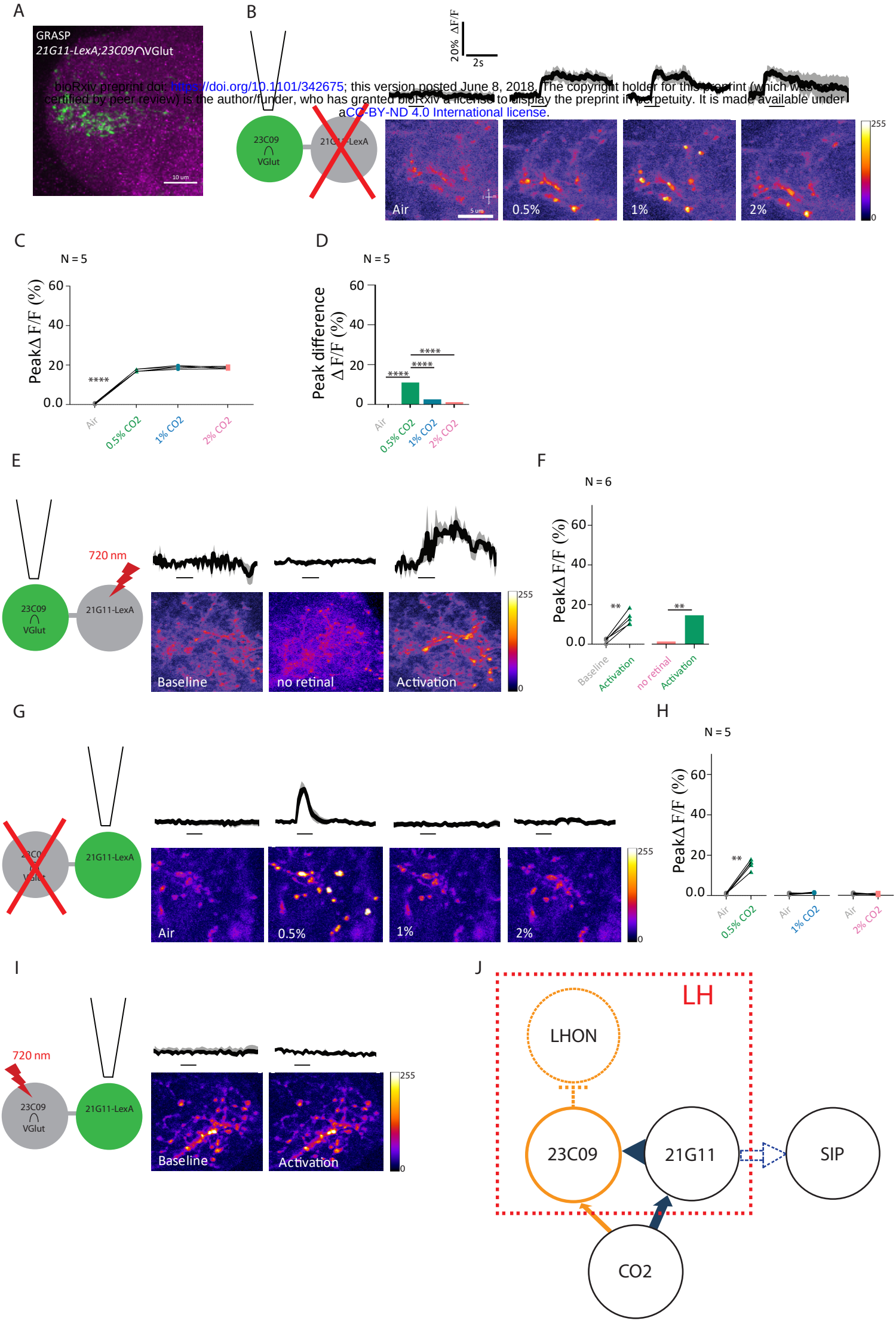

Figure 3
21G11LexA neurons are pre-synaptic to 23C09 ∩ VGlut neurons.

(A) Lateral horn showing GRASP, a measure of contact between the membranes of neurons, in 21G11-LexA and 23C09 ∩ VGlut.
(B) Schematics of the experiment and calcium response at the LH, using GCaMP6m, of 23C09∩VGlut neurons to air, 0.5%, 1% and 2% of CO2 while 21G11-LexA neurons are silenced by expression of Kir2.1.
(C and D) Peak GCaMP6.0m intensity change and peak difference in intensity after stimulation with air, 0.5%, 1% and 2% of CO2.
(E) Schematics of the experiment and calcium response at the LH of 23C09∩VGlut during baseline, activity without retinal and upon activation with 720 nm light of 21G11-LexA driving expression of Chrimson.
(F) Peak GCaMP6.0m intensity change of 23C09∩VGlut during baseline, activity without retinal and upon activation with 720 nm light of 21G11-LexA driving expression of Chrimson.
(G) Schematics of the experiment and calcium response at the LH, using GCaMP6m, of 21G11-LexA neurons to air, 0.5%, 1% and 2% of CO2 while 23C09∩VGlut neurons are silenced by expression of Kir2.1.
(H) Peak GCaMP6.0m intensity change after stimulation with air, 0.5%, 1% and 2% of CO2.
(I) Schematics of the experiment and LH activity of 21G11-LexA upon activation of 23C09∩VGlut neurons, expressing Chrimson, with 720 nm light.
(J) Proposed model of the LH neurons processing CO2 information.
For (B), (E), (G) and (I), on top it is shown the average time course of GCaMP6.0m intensity change. The black bar indicates the time of the stimulus. On bottom the representative images showing the pseudo-colored response. a=anterior; l=lateral; m=medial; p=posterior. Error bars indicate ±SEM **p<0.01, ****p<0.0001. All p values are calculated with Wilcoxon signed-rank test.

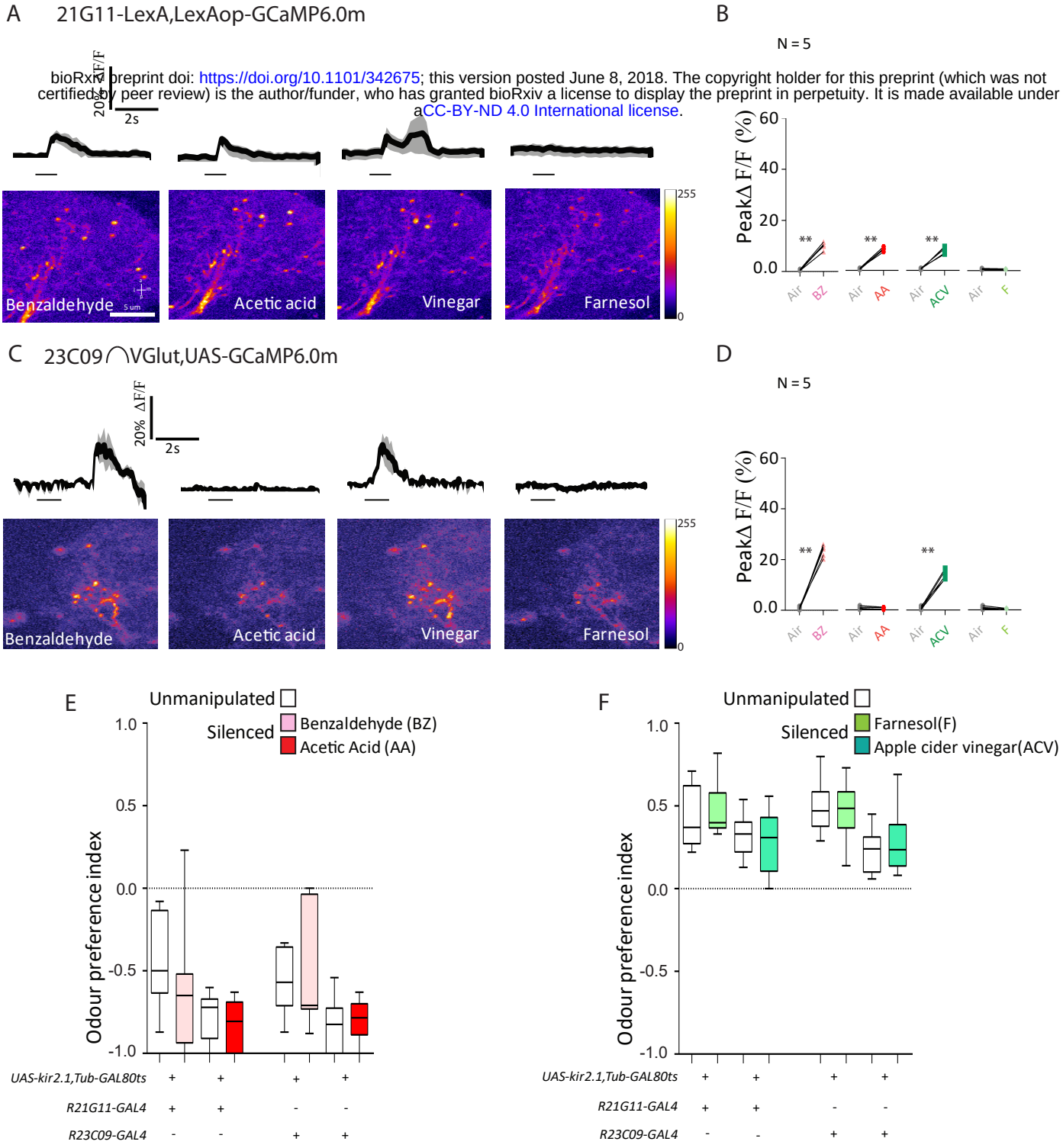

Figure 4
Physiological and behavioral response to attractive and repulsive compounds of R21G11 and R23C09 neurons

(A and C) Calcium response at the LH of 21G11-LexA and of 23C09∩VGlut to the repulsive compounds – benzaldehyde (BZ) and acetic acid (AA)- and the attractive compounds – farnesol (F) and apple cider vinegar (ACV). On top it is shown the average time course of GCaMP6.0m intensity change. The black bar indicates the time of the stimulus. On bottom the representative images showing the pseudo-colored response.
(B and D) Peak GCaMP6.0m intensity change after stimulation with benzaldehyde (BZ), acetic acid (AA), farnesol (F) and apple cider vinegar (ACV).
(E) T-maze response to benzaldehyde (BZ) and acetic acid (AA) of R21G11-GAL4 and R23C09-GAL4.
(F) T-maze response to farnesol (F) and apple cider vinegar (ACV) of 21G11-GAL4 and 23C09-GAL4.
(E-F) White boxes, no heat induction of Kir2.1 expression ("unmanipulated", see materials and methods). Colored boxes, heat induction of Kir2.1 expression before test ("silenced"). The box represents the first and the third quartiles and the whiskers the 10th and 90th percentiles. The line across the box is the median.
N=5 for A, B, C and D; N=10 for E and F. For B and D Error bars indicate ±SEM **p<0.01, ****p<0.0001. p values are calculated with Wilcoxon signed-rank test. For E and F comparisons calculated with one-way ANOVA are non-significant.